Indian Journal of Engineering & Materials Sciences
Vol. 15, April 2008, pp. 152-156

Impedance spectroscopy analysis of $(Pb_{0.93}Gd_{0.07})(Sn_{0.45}Ti_{0.55})_{0.9825}O_3$ ferroelectrics

B P Das[a*], R N P Choudhary[b] & P K Mahapatra[a]

[a]Department of Physics, Vidyasagar University, Midnapore 721 102, India
[b]Department of Physics and Meteorology, Indian Institute of Technology, Kharagpur 721 302, India

Received 7 November 2006; accepted 28 February 2008

The sample of $(Pb_{0.93}Gd_{0.07})(Sn_{0.45}Ti_{0.55})_{0.9825}O_3$ is prepared by a standard mixed oxide method. The prepared powder has been analyzed by XRD, and it is found to have tetragonal structure. The impedance spectrum analysis of $(Pb_{0.93}Gd_{0.07})(Sn_{0.45}Ti_{0.55})_{0.9825}O_3$ compound exhibits the appearance of single semicircular arc whose radii decreases gradually with increase in temperature. The bulk resistance at 425, 450, 475 and 500°C are found to be 325, 200, 130, 70 kΩ respectively. Nyquist plots ($Z^{//}$ versus $Z^{/}$) show the dominance of grain contribution, which allows the determination of relaxation frequency. The activation energy, calculated from the slope of lnτ versus $10^3/T$ plot, is found to be the nearly same as calculated from ac conductivity. The room temperature ac conductivity at 10 kHz lies in the range of 10^{-5}-10^{-6} ($ohm^{-1}m^{-1}$).

The synthesis and study of lead based compounds having perovskite structure has attracted large number of researchers since the discovery of ferroelectricity in $PbTiO_3$[1] in 1950s. These materials in the perovskite structure show high potential for device applications[2-5] due to their high spontaneous polarization (> 50 μC/cm^2), high dielectric constant above room temperature (T_c = 490°C) and high breakdown strength.

A useful technique to analyze the electrical properties of low conductivity materials and electroceramics is based on the study of complex impedance spectroscopy (CIS). Indeed, this technique offers several advantages such as the determination of relaxation frequency and separation of grain, grain-boundary and grain-electrode effects. These features will be particularly relevant for polycrystalline ferroelectric materials in general. The method is employed to analyze the properties of the intragranular and interfacial regions, their interrelations, and their dependence on such controllable variables as temperature, frequency and applied static voltage. The complex impedance spectroscopic studies involve measurement of real and imaginary parts of impedance for a wide range of frequency. In recent years, this technique has become a well-accepted fundamental tool for characterizing ionic conductors in terms of ionic conductivity, electrode polarization and activation energy for ion migration. Recently the method has been exploited to probe the solid electrolytes, particularly to distinguish the inter-grain, intra-grain conduction, micro-heterogeneity and electrode-material interface.

There is large number of literatures on electrical conductivity of ceramic-ceramic composites using CIS[6-15]. Impedance spectroscopy measurement for BST ceramics to study their PTCR behaviour was also reported[16]. Impedance spectroscopy measurement studies for other ferroelectric materials[17,18] were also used to gain an insight into the electrical mechanism inside those materials.

The literature survey reveals that the studies on the electrical properties of Gd substituted PST [i.e. $(Pb_{0.93}Gd_{0.07})(Sn_{0.45}Ti_{0.55})_{0.9825}O_3$] using complex impedance spectroscopy (CIS) technique received little attention. In the present study, we have carried out complex impedance formalism and relaxation process of the material.

Experimental Procedure

The polycrystalline sample of $(Pb_{0.93}Gd_{0.07})(Sn_{0.45}Ti_{0.55})_{0.9825}O_3$ was synthesized by a high-temperature solid-state reaction technique using high purity oxides: PbO (99% M/S Romali), SnO_2 (99% M/S Loba Chemical Co.), TiO_2 (99% M/S S. D. Fine Chem. Pvt. Ltd.) and Gd_2O_3 (99% M/S Indian Rare Earths Ltd.) weighed in the required stoichiometries and mixed them thoroughly in ethanol for 2 h. Then the mixtures were dried and calcined in an alumina crucible at 1000°C for 5 h in air. The fine

*For correspondence (E-mail: das_bhaktipada@yahoo.com)

and homogeneous material of the calcined powder was then mixed with a drop of the binder, 5% (w/w) aqueous polyvinyl alcohol solution. The granules are then pressed into disc type (cylindrical) pellets of 10 mm diameter and 1.40 mm thickness under an isostatic pressure of about 70 MPa using a hydraulic press in conventional cold pressing method. Polyvinyl alcohol (PVA) was used as binder to reduce the brittleness of the pellet. The organic binder was burnt out during high-temperature sintering at 1040°C for 3 h. To prevent PbO loss from pellet and to maintain the stoichiometry of the compound, equilibrium PbO vapour pressure was established by placing some amount of $PbZrO_3$ powder along with the pellets in a covered alumina crucible during high temperature sintering.

The formation of the desired compound was checked by preliminary X-ray structural study. X-ray diffractogram on calcined powder of Gd substituted PST [i.e. $(Pb_{0.93}Gd_{0.07})(Sn_{0.45}Ti_{0.55})_{0.9825}O_3$] in a wide range of Bragg angles, ($20^o \le 2\theta \le 80^o$) were recorded at room temperature using a Philips PW 1977. X-ray diffractometer with CuK_α radiation (λ = 1.5418Å) and a Ni filter operating at 40 kV and 20 mA, with a scanning rate of 2°/min. The prepared powder was analyzed by XRD technique and it was found to have tetragonal structure. However, a very small additional diffraction peak is observed around 29°, which cannot be indexed in the tetragonal structure. The intensity of this diffraction line is very small in comparison to the indexed diffraction lines and suggests the presence of a very small (less than 2%) amount of a secondary (pyrochlore) phase in the compound. The morphology of the surface was examined by SEM (Jeol, JSM 5800). Polycrystalline textures of the material with uniform grain distribution were observed throughout sample surfaces. The observed value of density of the prepared material was found to be 6.80 g/cc.

The flat polished surfaces of sintered pellets were electroded/painted with a high purity air-dried silver paste, and then cured 150°C for 2 h before taking any electrical measurements. The impedance analysis of the compound are carried out by the impedance measurement procedure using a computer controlled Hioki LCR Hi-tester (Model: 3532) at an ac signal level of amplitude 1.5 V in a wide range of temperature (room temperature to 500°C).

Results and Discussion

AC impedance methods are widely used for investigating the electrical behaviour of the materials over a wide range of frequency and temperature, which helps to separate the real and imaginary components of the electrical parameters and hence provide a better understanding of material characteristics. The impedance data $Z^*(\omega)$ were plotted in the complex plane, a representation based on the plot of the imaginary component Z'' versus the real component Z'. $Z^*(\omega)$ is represented by the equation $Z^*(\omega) = Z'(\omega) - jZ''(\omega)$. In complex impedance plane, each effect, viz., grain, grain boundary, or grain-electrode effect, appears as a semicircle, whose center lies on a line bellow the real axis. Each semicircle can then be assigned a value of *R* and *C*, which are connected in parallel.

Figure 1 shows complex impedance spectrum (Nyquist plots, i.e., Z'' versus Z' also called Cole-Cole plots) of the compound under investigation measured at different temperatures.

The impedance spectrum of $(Pb_{0.93}Gd_{0.07})(Sn_{0.45}Ti_{0.55})_{0.9825}O_3$ is characterized by the appearance of single semicircular arc whose radii

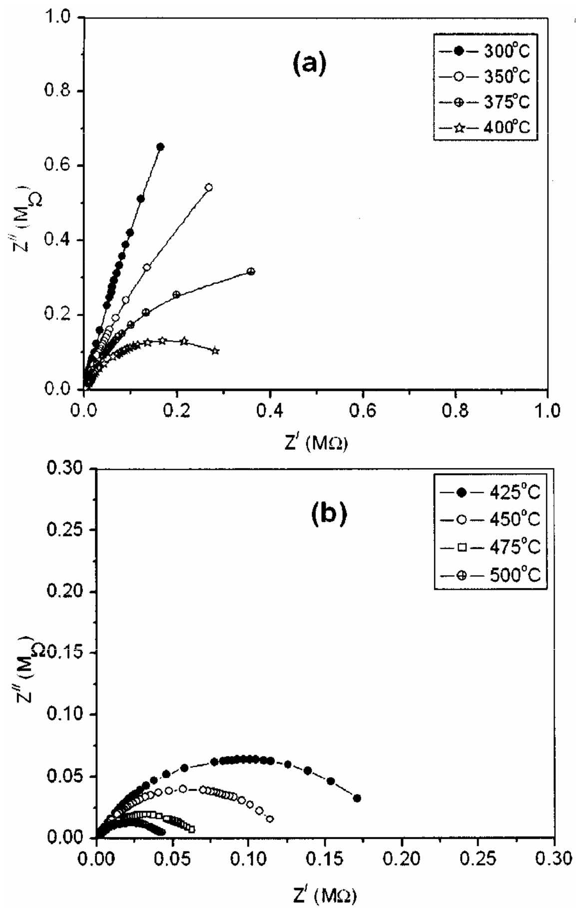

Fig. 1—Complex impedance spectrum of $(Pb_{1-x}Gd_x)(Sn_{0.45}Ti_{0.55})_{1-x/4}O_3$ at different temperatures

gradually decreases with increase in temperature. The intercepts of each semicircular arc with the real axis ($Z^{/}$) give us the bulk resistance of the material. The bulk resistance values at 425, 450, 475 and 500°C are 325, 200, 130, 70 kΩ respectively. And the corresponding bulk capacitance (C_g) values are 1.63×10^{-9}, 1.14×10^{-9}, 8.16×10^{-10}, 7.56×10^{-10} F. The corresponding relaxation times (τ_b) in this temperature range are 2.27×10^{-4}, 1.06×10^{-4}, and 5.30×10^{-5}, 3.53×10^{-5} s.

Only single semicircular arcs at all temperature indicate the dominance of grain effect other than the grain boundary and electrode effect. Single semicircular arcs of the impedance spectrum can be modeled as an equivalent circuit consisting of parallel combination of bulk resistance and bulk capacitance. The Nyquist plot shows that this semicircle exhibits some depression degree instead of a semicircle centered on the abscissa axis. This decentralization obeys Cole-Cole's formalism[20], where the depressed semicircle represents typically a phenomenon with a distribution of relaxation time. Cole-Cole formalism for complex impedance is given by:

$$Z^{*}(\omega) = \frac{R}{1+(j\omega/\omega_0)^{1-n}}$$

When n goes to zero ($1-n \rightarrow 1$) the above equation gives rise to the classical Debye's formalism. The values of n represent the magnitude of deviation from the ideal condition. The non-ideal behaviour is correlated to several factors such as grain size distribution, grain orientation and grain boundaries. The effect of the temperature on impedance behaviour of the sample becomes clearly visible from the pattern of the above plot. As the temperature increases, the intercept of the prominent semicircles on the $Z^{/}$ axis shift toward lower values $Z^{/}$, which indicates the reduction of grain, (grain boundary, interface resistance if exist) resistance. The decrease of bulk resistance of the material is more dominant at temperatures around 400-500°C. This may be due to ionic conduction, which is more dominant at higher temperature. The presence of single semicircular arc indicates that the electrical process in the material arises due to the contributions from bulk material.

Figure 2 shows the temperature dependence of bulk resistance (R_b). From the figures it is clear that the bulk resistance decreases sharply with rise in temperature up to temperature 600 K, and then decreases slowly. The rate of increase of bulk conductivity is different in different regions, which means different activation energies involved in different temperature regions for the bulk conductivity.

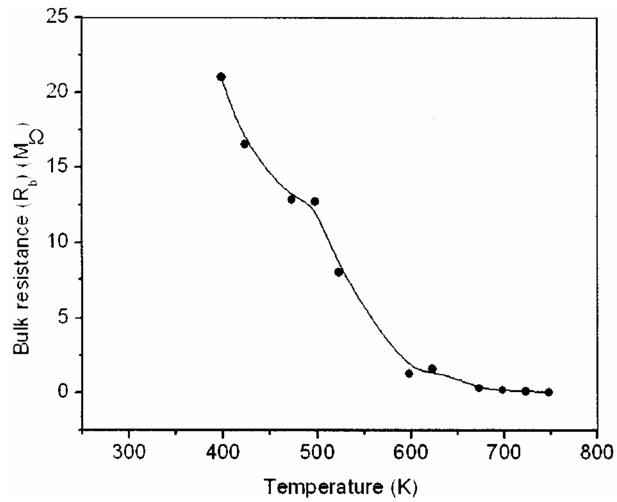

Fig. 2—Variation of bulk resistance with temperature $(Pb_{0.93}Gd_{0.07})(Sn_{0.45}Ti_{0.55})_{0.9825}O_3$ ceramics

Figure 3 shows the variation of real part of impedance ($Z^{/}$) with frequency at different temperatures of $(Pb_{0.93}Gd_{0.07})(Sn_{0.45}Ti_{0.55})_{0.9825}O_3$ compound. The magnitude of $Z^{/}$ decreases at lower frequencies with increasing temperature. At higher frequencies the value of $Z^{/}$ merges for all the temperatures of the sample. It is observed from the figures that $Z^{/}$ values decrease with increase of temperature indicating reduction of grains, grains boundaries and electrode interface resistance. This indicates the existence of negative temperature coefficient of resistance (NTCR) in the sample. The values of the real part of the impedance ($Z^{/}$) decreases up to a certain fixed frequency and then it remains almost constant value with increasing frequency.

Figure 4 exhibits variation of the imaginary part of impedance ($Z^{//}$) with frequency at different temperatures. The shift in the peaks of $Z^{//}$ towards higher frequency with increasing temperature is mainly due to change in relaxation in the sample. The asymmetric broadening of the peaks suggests the presence of electrical process of the material with spread of relaxation time (indicated by peak width). The relaxation species may be possibly due to presence of electron at low temperature and defects at higher temperature.

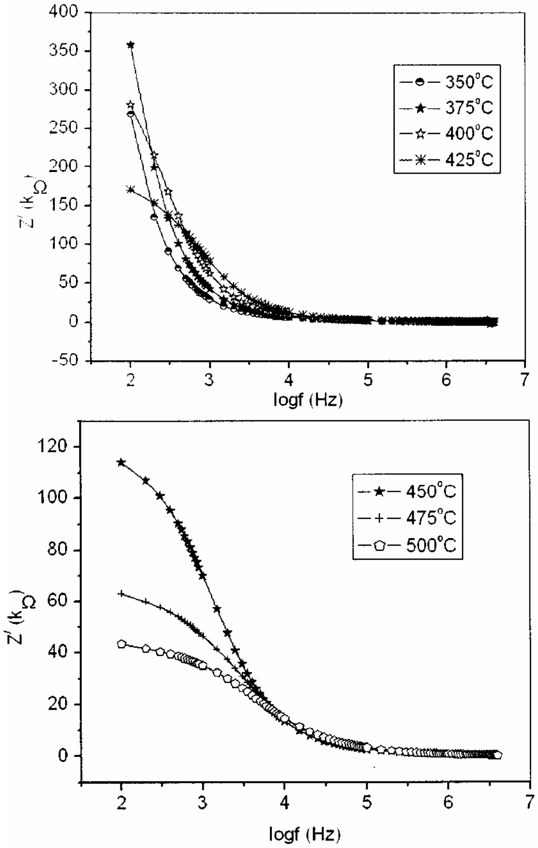

Fig. 3—Variation of real part of the impedance as a function of frequency at different temperatures of $(Pb_{0.93}Gd_{0.07})(Sn_{0.45}Ti_{0.55})_{0.9825}O_3$ ceramics

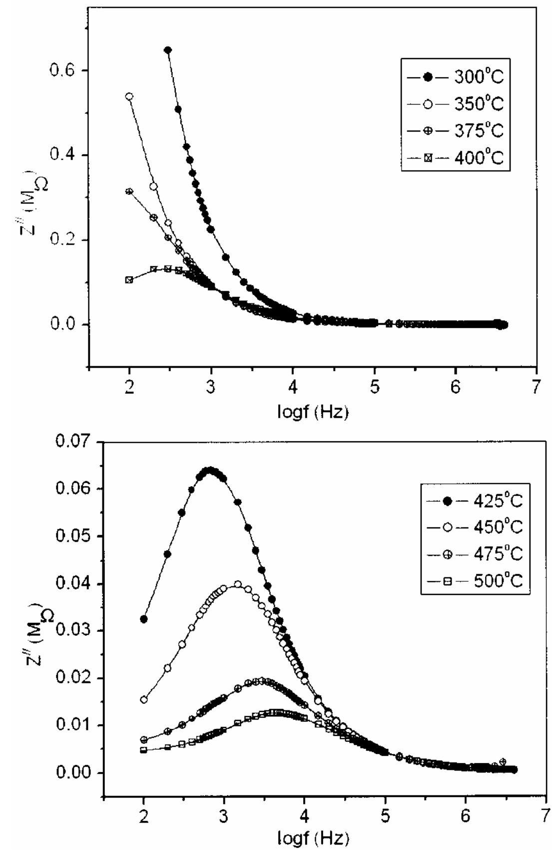

Fig. 4—Variation of imaginary part of the impedance as a function of frequency at different temperatures of $Pb_{0.93}Gd_{0.07})(Sn_{0.45}Ti_{0.55})_{0.9825}O_3$ ceramics

Figure 5 shows the variation of relaxation time ($\ln\tau$) with inverse of absolute temperature ($10^3/T$). The characteristic relaxation time (τ) was calculated from $Z^{//}$ versus $Z^{/}$ (and also from $Z^{//}$ versus log*f*) plots using the relation:

$$\tau = 1/\omega = 1/2\pi f_{\max}$$

where f_{max} is the relaxation frequency (frequency at which $Z^{//}$ was found to be maximum). It is observed that the value of relaxation time (τ) is found to be decreasing with increasing temperature, which represents semiconductor behaviour of the sample.

In polycrystalline samples, grains are semiconducting while the grain boundaries are insulating[21]. The semiconducting nature of the grains in ceramics is believed to be due to the loss of oxygen during high temperature sintering process.

The activation energy (E_a) of the compound under investigation is calculated using the Arrhenius' expression:

$$\tau = \tau_0 \exp(E_a/KT)$$

where τ_0 is the pre-exponential factor, K is Boltzamann constant and T is the absolute temperature. The activation energy is calculated from the slope of $\ln\tau$ versus $10^3/T$ plot. It has been observed that the activation energy for the material is found to be 1.34 eV.

In Fig. 6 behaviour of ac conductivity versus temperature is depicted for the $(Pb_{0.93}Gd_{0.07})(Sn_{0.45}Ti_{0.55})_{0.9825}O_3$ sample at a frequency of 10 kHz. Figure 6 shows that (i) σ_{ac} remain almost constant up to nearly 450 K, (ii) thereafter σ_{ac} increases with temperature up to the temperature at which the phase changes from ferroelectric to a paraelectric one, (iii) at the temperature of phase change a small resonant type anomaly occur and (iv) in the paraelectric phase σ_{ac} decreases. It is interesting to note that the slope of $\ln\sigma_{ac} \sim 1/T$ shows distinct variations for temperature below 450 K, 450 K to T_c and for $T > T_c$, which means different

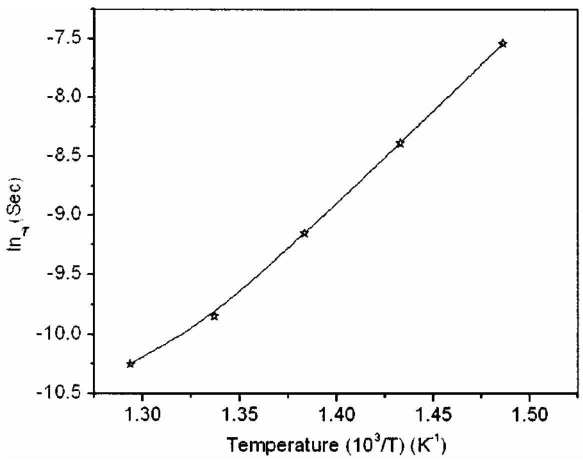

Fig. 5—Variation of relaxation time (τ) with temperature

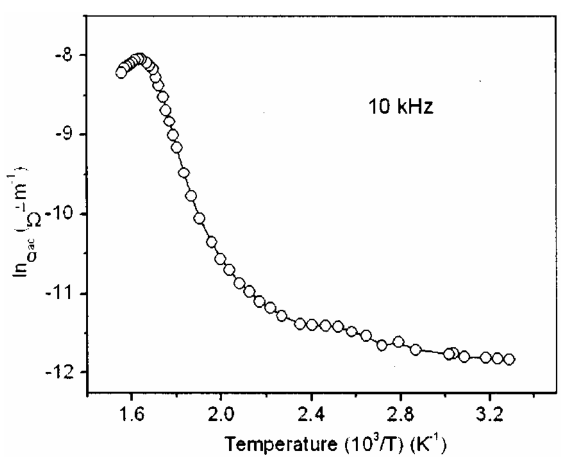

Fig. 6—Temperature variations of ac conductivity of $(Pb_{0.93}Gd_{0.07})(Sn_{0.45}Ti_{0.55})_{0.9825}O_3$ ceramics at 10 kHz

activation energies involved in different temperature regions in the conduction process. The room temperature ac conductivity at 10 kHz lies in the range of 10^{-5}-10^{-6} (ohm^{-1}m^{-1}).

Conclusions

The substitution of Gd^{3+} ions at the Pb^{2+} sites of $(Pb_{0.93}Gd_{0.07})(Sn_{0.45}Ti_{0.55})_{0.9825}O_3$ compound do not alter the basic structure of $Pb(Sn_{0.45}Ti_{0.55})O_3$ sample, which crystallizes in tetragonal structure. However, the extra diffraction peak observed around 29° suggest the presence of a very small (less than 2%) amount of a secondary (pyrochlore) phase in the compounds. Complex impedance analysis of the material reveals the dominance of grain effect other than the grain boundary and electrode effect. The magnitude of Z' decreases at lower frequencies with increasing temperature indicating reduction of grains, grains boundaries and electrode interface resistance. This indicates the existence of negative temperature coefficient of resistance (NTCR) in the sample. A significant broadening of the peaks with rise in temperature suggests the presence of temperature dependent relaxation process of the material. The decrease of relaxation time (τ) with increasing temperature represents the semiconductor behaviour of the sample. In polycrystalline samples, grains are semiconducting while the grain boundaries are insulating. The semiconducting nature of the grains in ceramics is believed to be due to the loss of oxygen during high temperature sintering process.

Acknowledgements

One of the authors (B P Das) gratefully acknowledges Prof. P K Biswas, Mr A Mukhopadhyay and Dr A K Thakur, IIT, Kharagpur for their valuable suggestions.

References

1 Shirane G, Hoshino S & Suzuki K, *Phys Rev,* 80 (1950) 1105.
2 Jaffe B, Roth R S & Marzullo S, *J Appl Phys,* 25 (1954) 809.
3 Herbert J M, *Ferroelectric Transducers and Sensors* (Gordon and Breach, London), 1982.
4 Newnham R E & Ruschau G R, *Am Ceram Soc Bull,* 75(10) (1996) 51.
5 Smith W D & Land C E, *Appl Phys Lett,* 20 (1972) 169.
6 Jonscher A K, *Nature*, 267 (1977) 673.
7 Sluyters J H, *Acta Electrochem,* 11 (1965) 483.
8 Bauerle J E, *J Phys Chem Solids,* 30 (1969) 2657.
9 Almond P, West A R & Grant G R, *Solid State Commun*, 44 (1982) 1277.
10 Macdonald J R & Brachman M R, *Mod Phys*, 28 (1956) 393.
11 Mayer J, *Phys Chem*, 90 (1986) 26.
12 Naohiro H & West A R, *J Am Ceram Soc*, 79(6) (1996) 1633.
13 Sakamoto S, Yoshinaka M, Hirota K & Yamaguchi O, *J Am Ceram Soc*, 80(1) (1997) 267.
14 Rahaman A K & Susan C M Schneider & Martin A S, *J Am Ceram Soc,* 80(5) (1997) 1198.
15 James A R & Srinivas K, *Mater Res Bull*, 34 (1999) 114.
16 Viviani M, Nanni P, Buscaglia M T, Leoni M., Buscaglia V & Centurioni L, *J Eur Ceram Soc*, 19 (1999) 781.
17 Reau J M, Annie S, Mohamed O E & Ravez J, *J Eur Ceram Soc*, 19 (1999) 777.
18 Bennani F & Husson E, *J Eur Ceram Soc,* 21 (2001) 847.
19 Sinclair D C & West A R, *J Appl Phys*, 66 (1989) 3850.
20 Cole K S & Cole R H, *J Chem Phys,* 9 (1941) 341.
21 Singh S P, Singh A K & Pandey D, *J Mater Res,* 18 (2003) 1.